Available online at www.sciencedirect.com
SCIENCE DIRECT®
International Journal of Heat and Fluid Flow 26 (2005) 156–172
International Journal of HEAT AND FLUID FLOW
www.elsevier.com/locate/ijhff

Pressure drop, gas hold-up and heat transfer during single and two-phase flow through porous media

M. Jamialahmadi [a], H. Müller-Steinhagen [b,c,*], M.R. Izadpanah [d]

[a] University of Petroleum Industry, Ahwaz, Iran
[b] Institute for Thermodynamics and Thermal Engineering, University of Stuttgart, Pfaffenwaldring 38–40, Stuttgart 70569, Germany
[c] Institute of Technical Thermodynamics, German Aerospace Center (DLR), Germany
[d] The School of Engineering, University of Kerman, Kerman, Iran

Received 23 October 2003; accepted 22 July 2004
Available online 23 September 2004

Abstract

Pressure drop, bubble size, gas hold-up and convective heat transfer have been studied both experimentally and theoretically at constant wall heat flux for single and two-phase flow through unconsolidated porous media. Single-phase pressure drop and heat transfer coefficients have been measured over a wide range of particle size, heat flux and liquid flow rate. The conservation equations and the Kozeny-Carman equation are used to describe single-phase flow pressure drop and convective heat transfer through the porous media. The measured pressure drops have been used to evaluate the validity of the predictive expressions available in the literature. Mathematical models are developed for the prediction of temperature profiles and single-phase heat transfer coefficients, which predict the experimental data with good accuracy. A large number of new experimental data are presented on two-phase pressure drop, bubble size, gas hold-up and heat transfer coefficients for co-current upward gas/liquid flow through beds of different particle sizes under constant wall heat flux. The experimental data suggest the existence of two distinct regimes, i.e. homogeneous and heterogeneous flow. The experimental data on two-phase pressure drop and gas hold-up have also been compared with the prediction of published correlations. Finally, mathematical models are presented for the prediction of pressure drop, bubble size, gas hold-up and heat transfer which predict the experimental data with good accuracy.

1. Introduction

Single and two-phase gas/liquid flow through porous media composed of stationary granular particles is frequently encountered in many diverse fields of science and engineering, ranging from agricultural, biomedical, mechanical, chemical and petroleum engineering to food and soil sciences. Classical research areas of chemical engineering dealing with porous media include filtration, drying, and multi-phase flow in packed columns and catalytic reactors. In all these instances it is necessary to predict design parameters such as friction factor, pressure drop, bubble size, gas hold-up, heat and mass transfer coefficients in order to determine the desired operating conditions and the size of the equipment required for the specific purposes. Therefore, expressions are needed to predict these parameters accurately in porous media in which fluids are flowing either alone or as gas/liquid mixtures. In the last decade there has been a steady effort, both experimentally and theoretically, to improve the knowledge of single-phase flow and heat transfer in porous media. These studies have been reviewed by several investigators (e.g. Combarnous and Bories, 1975; Cheng, 1978; Stankiewicz, 1989; Tien and Vafai, 1990). In most cases, Darcian flow was

* Corresponding author. Address: Institute for Thermodynamics & Thermal Engineering, University of Stuttgart, Pfaffenwaldring 38–40, Stuttgart 70569, Germany. Tel.: +49 711 6862 358; fax: +49 711 6862 712.
E-mail address: hans.mueller-steinhagen@dlr.de (H. Müller-Steinhagen).

0142-727X/$ - see front matter © 2004 Elsevier Inc. All rights reserved.
doi:10.1016/j.ijheatfluidflow.2004.07.004

Nomenclature

a	total surface area of the particles, m^2
C_n	defined by Eq. (24)
c_{pg}	gas phase heat capacity, J/kg K
c_{pl}	liquid phase heat capacity, J/kg K
d_b	bubble diameter, m
d_c	test section diameter, m
d_p	pore diameter, m
d_r	the ratio of bubble and particle size
d_s	particle diameter, m
D_e	characteristic length defined by Turpin and Hungtington
f	friction factor
$F(u_r, d_r)$	defined by Eq. (14)
g	gravitational acceleration, m^2/s
G	gas phase mass flow rate, kg/m^3
h	heat transfer coefficient, $W/m^2 K$
J_0, J_2	Bessel functions
k	permeability, m^{-2}
L	length, m or liquid mass flow rate, kg/m^3
L_b	bubble length, m
m	constant
P	pressure, Pa
$\dot{q}$	heat flux, W/m^2
r	radial distance, m
r_0	radius of bed, m
Re	Reynolds number, $\rho U d_s/\mu$
Re_m	Modified Reynolds number, $\rho u d_s/\mu(1-\delta)$
s	distance between thermocouple in the wall and inner surface, m
T	temperature, K
T_b	bulk temperature
T_C	center temperature, K
T_{TC}	thermocouple temperature, K
T_0	initial temperature, K
T_S	surface temperature, K
u_f	fluid velocity, m/s
u_{sg}	superficial gas velocity, m/s
u_{sl}	superficial liquid velocity, m/s
u_P	fluid velocity in a single pore, m/s
u_r	The ratio of superficial gas and liquid velocities
x	distance, m

Greeks

ΔP_f	pressure drop, Pa
χ	Lockhart–Martinelli parameter
Γ	effective thermal diffusivity of gas/liquid systems, m^2/s
Λ	separation constant
α_e	effective single-phase thermal diffusivity, m^2/s
δ	bed porosity
ε_g	gas hold-up
ε_l	liquid hold-up
γ	constant
λ	thermal conductivity, W/m K
μ	viscosity, kg/m s
ρ	density, kg/m^3
σ	surface tension, N/m

Subscripts/Superscripts

b	bubble or bulk
c	forced convection or column
e	effective
es	effective, single-phase
et	effective, two-phase
f	fluid
g	gas phase
l	liquid
m, g	modified gas phase
m, l	modified liquid phase
os	stagnant, single-phase
ot	stagnant, two-phase
p	pore
s	solid or single-phase
sg	superficial velocity
sl	superficial liquid velocity
t	two-phase or total
TC	thermocouple
w	wall

assumed; however, some researchers have extended their work into non-Darcian flow as well (e.g. Vafai and Tien, 1981; Hunt and Tien, 1988). Several studies concentrate on property variations of the bed, such as porosity and their effect on the heat transfer process (Vafai et al., 1985). A comprehensive review of these investigations can also be found in the books of Bear and Bachmat (1990), Kawiany (2002) and Nield and Bejan (1999). Several correlations have been recommended for the prediction of pressure drop and heat transfer in porous media saturated with fluids. Although these models can describe the hydrodynamics of single-phase flow quite well, there are nevertheless some disagreements in the predictions. The studies on single-phase heat transfer have mostly dealt with a gaseous medium as the saturating fluid and constant wall temperature boundary condition. The available information on heat transfer under constant wall heat flux and in the non-Darcian regime is inadequate.

Much less information is available on hydrodynamics and heat transfer of two-phase gas/liquid flow through porous media. Two-phase flow through porous media

is an important area, which covers a broad spectrum of engineering disciplines including geothermal systems (Sondergeld and Turcotte, 1977; Cheng, 1978), oil reservoir engineering (Scheidegger, 1974; Bear, 1972), post-accident analysis of nuclear reactors (Lipinski, 1981; Tung and Dhir, 1988), multi-phase packed bed reactors (Shah, 1979), condensation enhancement and thermal energy storage (Plumb et al., 1990; Vafai and Sözen, 1990). Many attempts have been made to identify the flow regimes encountered when gas and liquid flow concurrently through porous media (Larkins and White, 1961; Eisenklam and Ford, 1962; Turpin and Huntington, 1967). These investigators observed different flow regimes, namely the homogeneous, transition and heterogeneous regimes, by establishing a constant liquid flow rate through the bed and then increasing the gas flow rate. They correlated the frictional pressure drop according to a Lockhart–Martinelli approach based on the knowledge of single-phase frictional losses for the gas and the liquid phase flowing alone in the bed. Comparison of the correlation by Turpin and Huntington (1967) with Larkins and White (1961) data shows differences of 30–50%. Saada (1972) used data of Eisenklam and Ford (1962) to construct a flow diagram of two-phase flow through beds of finely divided particles. Khan and Varma (1997) also presented their experimental data in the form of a flow map and then compared their results with those reported by Saada (1972). They concluded that the map suggested by Saada is inadequate for identifying the various flow regimes in packed beds. Khan and Varma (1997) also presented different correlations for frictional pressure drop for each flow regime and argued that separate correlations for the different regimes were advantageous when compared to the correlation of Turpin and Huntington (1967). Goto and Gaspillo (1992) studied gas/liquid flow through small packing material and presented correlations to predict frictional pressure drop in a manner similar to that of Lockhart and Martinelli. They used the Ergun (1952) correlation to estimate the single-phase pressure drop in packed beds. A general alternative description of two-phase flow has been proposed by Hassanizadeh and Gray (1988, 1993). They emphasized that the averaging of microscopic drag forces leads to a macroscopic non-linear theory for flow, but that the average of microscopic inertial terms is negligible in typical practical circumstances. Avraam and Payatakes (1995) studied two-phase flow in porous media using a micro-model pore network of the chamber-and-throat type, etched into glass. During each experiment, the pore-scale flow mechanisms were observed, the mean water saturation was determined with image analysis and the corresponding relative permeabilities and fractional flow have been calculated.

The subject of two-phase heat transfer in porous media has gained considerable attention during the last few years. The studies mostly concentrate on drying of different porous media, condensation in porous media, heat pipe application and geothermal applications. Dybbs and Schweitzer (1973) formulated the problem of non-isothermal flow in porous media for low Reynolds number where the inertia term is negligible. Dinulescu and Eckert (1980) studied the problem of mixture migration due to a temperature gradient in porous media. They performed a one-dimensional analysis of this problem and produced an analytical solution. Lyczkowski and Chao (1984) reported studies on two-phase drying. In their work, the effect of non-condensable components is not taken into consideration. Several authors have used a one-dimensional model to analyze condensation in porous media (i.e. Nilson and Romero, 1980; Ogniewicz and Tien, 1981; Vafai and Sarkar, 1987). The problem studied consists of a porous slab subjected to different environments on two sides. Vafai and Whitaker (1986) also studied a different problem using a two-dimensional transient model. Laminar film condensation in a porous medium was analyzed by White and Tien (1987a,b). The non-slip boundary condition was employed for the velocity at the wall and an exponential function for the porosity. Sözen and Vafai (1990) analyzed the transient forced convective condensing flow of a gas through a packed bed, with quadratic drag effects incorporated. The effects of thermal non-equilibrium in connection with the condensing flow of a vapor have been included in numerical simulations by Sözen and Vafai (1993), Amiri and Vafai (1994) and Amiri et al. (1995). They found that the local thermal equilibrium condition was dependent on particle Reynolds number and independent of thermophysical properties.

A literature review on heat transfer during two-phase flow in porous media and packed beds reveals that most research which had been carried out in this area was directed towards phase change in porous media, where the entering flow is usually a liquid or a vapor. Published correlations are based on the energy equation which is solved either analytically or, in most cases, numerically under constant wall temperature. However, there is little information on heat transfer in porous media with two-phase flow as the feed. Zhukova et al. (1990) undertook a thorough review of the literature on two-phase gas/liquid flow in stationary beds and concluded that research on heat transfer with ascending gas/liquid flow through porous media under constant wall heat flux was practically non-existent. In order to obtain prediction models for pressure drop, bubble size, gas hold-up and heat transfer for co-current two-phase gas/liquid upward flow through packed beds of fine particles under constant wall heat flux, there is need for better understanding of the role of the various operating parameters and of the mechanisms of heat transfer. The principal aim of the present investigation was to measure pressure

drop, bubble size, gas hold-up and heat transfer coefficients in packed beds over a wide range of superficial gas and liquid velocities, heat fluxes and solid particle physical properties. The predictions of various correlations from the literature are compared with these experimental data. Theoretical models are presented for the prediction of pressure drop, bubble size, gas hold-up and heat transfer coefficients to correlate the presented experimental data.

2. Experimental equipment and procedure

2.1. Test rig

Fig. 1 illustrates the schematic diagram of the experimental set-up. The basic components of the test rig are the test section, the peristaltic pump, tank, flow meter and gasometer. The stainless steel test section is 32 mm in diameter and 580 mm long. The tube was packed with glass beads of different diameters hence forming porous media with different system pore size distribution. Six pressure transducers are installed at equal distances along the bed, which can measure pressures up to 4 bar with very high accuracy. At the inlet and outlet of the test section two knit-meshes are kept in place by flanges, which contain the particles and prevent them from leaving the bed. All tubing and fittings are made of stainless steel. For those experiments, where flow patterns and gas hold-up have been investigated, the stainless steel test section was replaced by a perspex test section with a diameter of 37 mm and a length of 600 mm. The liquid is pumped from the reservoir tank to the test section using a peristaltic pump. Adjusting the revolutions of the pump controls the flow rate of the liquid phase. The gas phase flows from a compressor via a filter and pressure regulator to the test section. The air flow rate is adjusted by a flow meter at the inlet of the bed and measured again precisely at the outlet using an online gasometer. For the two-phase flow measurements, the two fluids are mixed shortly before the test section.

Heating is achieved by a Thermocoax resistance heating wire which is placed in a spiral groove around the pipe and embedded by high temperature soldering tin to ensure good contact with the test section wall. The bed extends above and below the heated section to ensure uniform distribution of the flow. Longitudinal grooves accommodate thermocouples measuring the wall temperatures. The local temperature of the wall is measured using thermocouples, which are located close below the heat transfer surface. The ratio between the distance of the thermocouples from the heat transfer surface and the thermal conductivity of the wall material $(s/\lambda)_w$ was determined by calibration measurements using the Wilson plot technique. The heat transfer surface temperature can be calculated using this ratio, the heat flux and the thermocouple temperature.

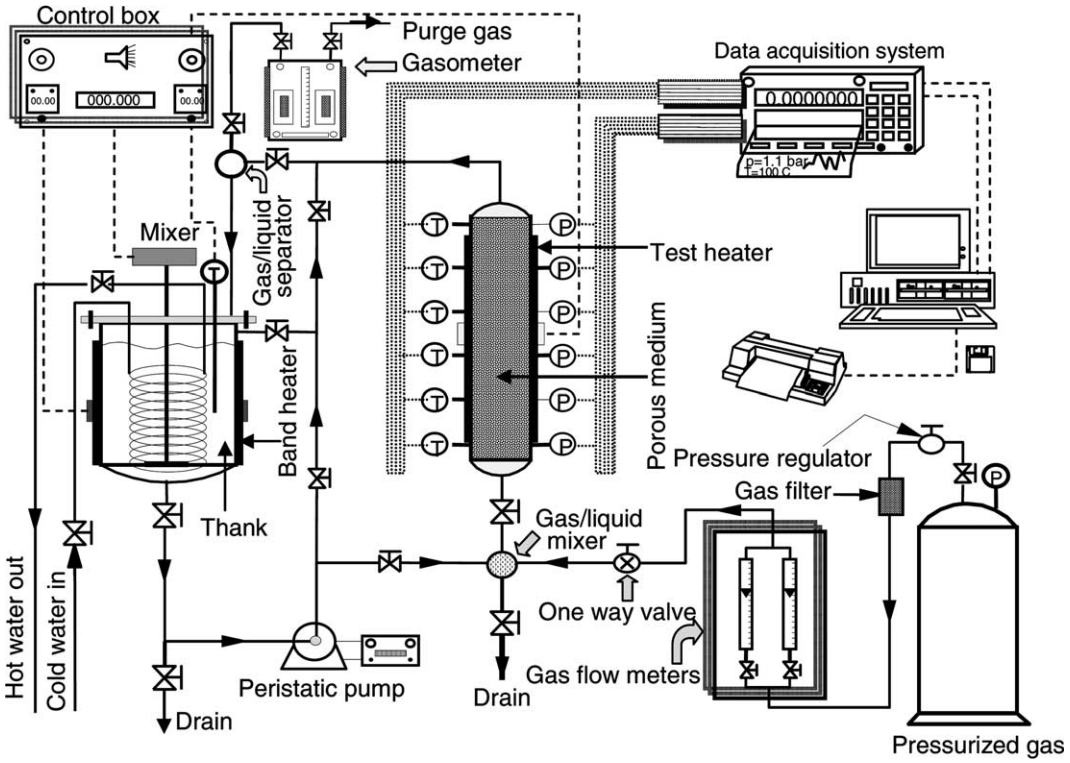

Fig. 1. Porous medium test apparatus.

$$T_S = T_{TC} - \frac{\dot{q}}{(s/\lambda)_w} \quad (1)$$

Bulk temperature is measured using six thermocouples which are inserted along the length of the bed. Another eight thermocouples are used to measure the wall temperature at two different positions along the bed. All signals are fed into a data acquisition system which is connected to a desk top computer. The gas and liquid phases used in this investigation were air and distilled water, respectively. The physical properties of the fluids and the particles are given in Table 1.

2.2. Experimental procedure and data reduction

To start the experiments, clean and dried preweighted particles of a given size are poured into the test section and placed into a shaker for 1 h. Then the bed is leveled, its height recorded and the test section installed back to its position in the test loop. Initially only liquid is pumped through the bed, and then the gas flow is gradually raised while the liquid flow rate is kept constant. The power supply to the test heater is then switched on and maintained at a predetermined value. Before any readings are taken, the system is left to itself for about 1 h to establish homogeneous and steady-state conditions throughout. Finally, the data acquisition system is started to record pressures, heat flux, temperatures, gas and liquid flow rates. Gas hold-up is measured using the bed expansion method. This technique relies on the instantaneous isolation of the bed from both liquid and gaseous feed. This is achieved by the use of quick action isolation valves on both gas and liquid inlets. It is assumed that the difference in the liquid level is produced by the gas hold-up in the system; according to the definition that gas hold-up is the fraction of the volume occupied by the gas bubbles. All experimental runs were performed with gradually increasing air flow rate while keeping the water flow rate constant. The local heat transfer coefficients are defined as:

$$h = \frac{\dot{q}}{T_S - T_C} \quad (2)$$

Table 2
Range of operating parameters

Liquid velocity	0.004–0.7 cm/s
Gas velocity	0–30 cm/s
Heat flux	1000–5000 W/m^2
Bulk temperature	20–90 °C
Inlet temperature	20–30 °C
System pressure	1–2 bar

The power supplied to the test heater is calculated from the measured current and voltage drop. The average of five thermocouple readings is used to determine the difference between wall and bulk temperature for each location.

The experimental runs were performed in an arbitrary sequence and some experiments were repeated to check the reproducibility of the experiments, which proved to be good. The range of experimental parameters covered in this investigation is summarized in Table 2.

3. Experimental results

3.1. Single-phase flow

In single-phase flow, the pressure gradient across the bed is a function of system geometry, bed porosity, bed permeability and physical properties of the liquid phase. Considerable progress has been made in establishing the velocity–pressure drop relationship and several correlations have been developed to describe the hydrodynamics of these with acceptable accuracy. Some of these models are summarized in Table 3. The Kozeny-Carman model (1927) is still the most widely used correlation for the prediction of pressure drop and recommended in almost all chemical engineering books for Darcian and non-Darcian flow regimes. Darcy's model is universally used for fluid flow through porous media in oil reservoir engineering and in almost all reservoir simulators.

Pressure drop was measured at six positions along the porous medium in the direction of flow, for a range of liquid velocities. Typical measurements for single-phase,

Table 1
Physical properties of packing material and fluids

Materials	d_s (mm)	δ	K (m^{-2})	ρ_s (kg/m^3)	μ (kg/m s)	λ_s (W/mK)
Glass beads	3	0.38	1.7×10^{-9}	2500	–	1.05
	1.5	0.367	1.0×10^{-9}	2500	–	1.05
	1	0.365	0.79×10^{-9}	2500	–	1.05
	0.4–0.6	0.362	1.71×10^{-10}	2500	–	1.05
	0.18–0.25	0.361	8.56×10^{-11}	2500	–	1.05
Mineral sand	0.25–0.425	0.375	4.62×10^{-11}	2300	–	5.34
Distilled water	–	–	–	996	0.798×10^{-3}	0.613
Air	–	–	–	1.1774	0.0000184	0.026

Table 3
Correlations suggested for the prediction of single- and two-phase flow pressure drop

Reference	Correlation
Darcy (1856)	$\frac{\Delta P}{L}=\frac{\mu}{k}\cdot u_f$ Single-phase, Darcian flow regime
Blake (1922)	$\frac{\Delta P}{L}=\frac{k\mu a}{g}\cdot\frac{G^2}{g_c\rho_f}\cdot\frac{a}{\delta^3}$ Single-phase, Darcian and non-Darcian flow regimes
Kozeny-Carman (1927)	$\frac{\Delta P}{L}=\frac{150(1-\delta)^2}{d_s^2\delta^3}\mu_f\cdot u_f+\frac{1.75(1-\delta)}{\delta^3 d_s}\cdot\rho u_f^2$ Single-phase Darcian and non-Darcian flow regimes
Leva (1947)	$\frac{\Delta P}{L}=\frac{k(1-\delta)}{g_c\delta^3}\left(\frac{d_sG}{\mu}\right)^{1.9}\cdot\left(\frac{\mu^2\chi^{1.1}}{\rho d_s^3}\right)$ Single-phase, Darcian and non-Darcian flow regimes
Ergun (1952)	$\frac{\Delta P}{L}=\frac{150(1-\delta)^2}{d_s^2\delta^3}\mu_f\cdot u_f+\frac{1.75(1-\delta)}{\delta^3 d_s}\cdot\rho u_f^2$ Single-phase, Darcian and non-Darcian flow regimes and for $\frac{Re_{m,g}}{1-\delta}=1-2000$
Larkins and White (1961)	$\log\left(\frac{\Delta P_t/L}{\Delta P_l/L+\Delta P_g/L}\right)=\frac{0.416}{(\log\chi)^2+0.666}$ where $\chi=\left(\frac{\Delta P_l}{L}/\frac{\Delta P_g}{L}\right)^{0.5}$ Two-phase gas/liquid flow for homogeneous and heterogeneous flow regimes
Ford (1960)	$\frac{\Delta P_t}{L}=\frac{0.0407g\rho_l\mu_l}{\mu_g}\cdot Re_l^{0.29}\cdot Re_g^{0.57}$ Two-phase air/water flow, for $d_s=1$ mm and $d_c=4.52$ cm
Turpin and Huntington (1967)	$\frac{\Delta P_t}{L}=\frac{2\rho_g u_{sg}^2}{D_c g_c}\cdot f_t$ where $\ln f_t=8-1.12\ln Z-0.0769(\ln Z)^2+0.0152(\ln Z)^3$, $Z=\frac{Re_g^{1.167}}{Re_l^{0.767}}$ Two-phase flow and for $\left(\frac{L}{G}\right)^{0.24}=1$–5 and $\frac{Re_g^{1.167}}{Re_l^{0.767}}=0.1$–1000
Saada (1972)	$\frac{\Delta P_t}{L}=0.027g\rho_l Re_l^{0.35}Re_g^{0.51}\left(\frac{d_c}{d_s}\right)^{1.15}$ Two-phase flow and for $Re_l=2.1$–153.2 and $Re_g=15$–600
Goto and Gaspillo (1992)	$\frac{\Delta P_t}{L}=y\cdot\left(\frac{\Delta P_l}{L}+\frac{\Delta P_g}{L}\right)$ where $\ln y=\frac{0.55}{\ln(\chi/1.2)^2+0.666}$ Two-phase flow, homogeneous and heterogeneous flow regimes
Khan and Varma (1997)	$\frac{\Delta P_t}{L}=\frac{u_{sl}^2\rho_l}{2d_s}\cdot f$ where, For bubbly flow: $f=3\times10^7 Re_g^{0.18}Re_l^{-1.7}\left(\frac{d_s}{d_c}\right)^{1.5}$ For pulse flow: $f=2.36\times10^7 Re_g^{0.26}Re_l^{-1.7}\left(\frac{d_s}{d_c}\right)^{1.5}$ For spray flow: $f=3.91\times10^5 Re_g^{1.12}Re_l^{-1.82}\left(\frac{d_s}{d_c}\right)^{1.5}$ Two-phase flow, bubbly, pulse and spray flow regimes

liquid flow are depicted in Fig. 2. A linear relationship exists between pressure drop and distance in the direction of flow in the bed. The slope of this proportionality increases sharply as the liquid velocity increases. Fig. 3 shows a typical comparison between measured and predicted pressure drops for a bed packed with 0.5 mm particles as a function of modified liquid phase Reynolds number $Re_{m,l}$. While all correlations predict an increase in pressure drop with increasing liquid velocity, the variation between the actual values from the different correlations is quite considerable. The best agreement between measured and calculated values is obtained with the correlations suggested by Kozeny-Carman (1927) and by Ergun (1952) for both, the Darcian and non-Darcian flow regime. As expected Darcy's model can predict the experimental data only at low liquid

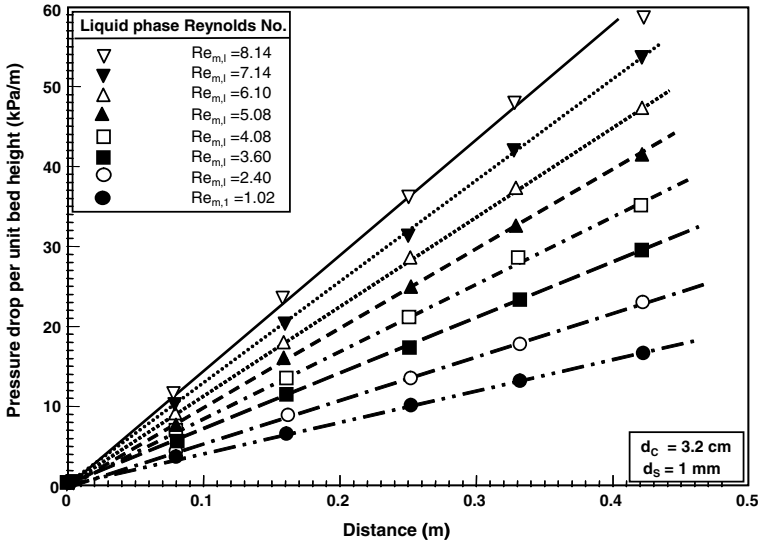

Fig. 2. Pressure drop along the porous medium.

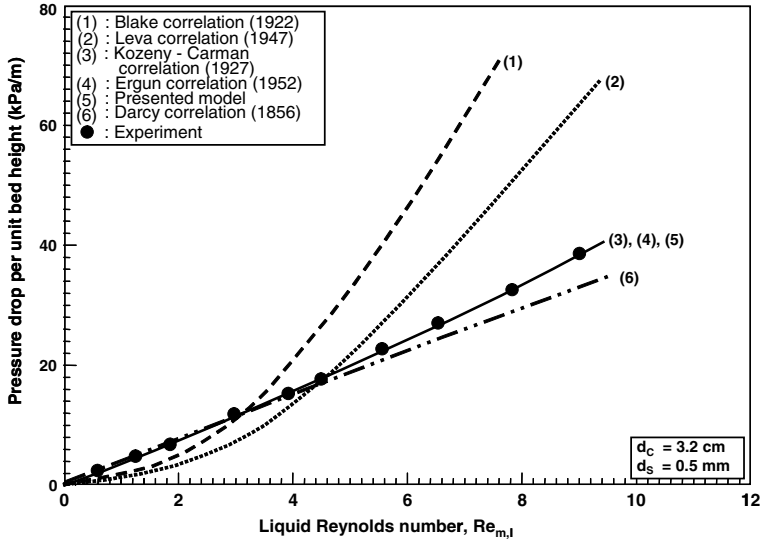

Fig. 3. Prediction of single phase pressure drop from various correlations.

Reynolds numbers. Despite the substantial similarity in the end results, the Kozeny-Carman correlation is a semi-empirical model based on a cylindrical pore model, whereas the Ergun equation is purely empirical. The Kozeny-Carman correlation predicts the present experimental data with an absolute mean average error of about 3.5%. This semi-empirical correlation is expressed as follows:

$$\frac{\Delta P_f}{L} = \frac{150(1-\delta)^2}{\delta^3 d_s^2}\mu_f \cdot u_f + \frac{1.75(1-\delta)}{\delta^3 d_s}\rho_f u_f^2 \tag{3}$$

Eq. (3) is a form of the Forchheimer (1901) equation for homogeneous packed beds of fine particles and unidirectional flow (Nield and Bejan, 1999). The two terms on the right hand side of Eq. (3) can be recognized as viscous and inertial contributions. At low Reynolds numbers the second term is negligible and Eq. (3) reduces to Darcy's equation. At high Reynolds numbers, when the fluid inertia is important, the second term becomes dominant.

3.2. Two-phase flow

3.2.1. Flow pattern

Contrary to single-phase flow, the problem of pressure drop during two-phase, gas/liquid flow in porous media is still largely unresolved. Fig. 4 is a schematic representation of visual and photographical observations. At a constant liquid velocity, two different regimes may be distinguished, as the superficial gas velocity is increased from 0 to 20 cm/s. At low gas velocities, a homogeneous flow regime prevails and the tiny bubbles pass through the bed without significant collisions or coalescence. Since they flow at almost the same velocity as the liquid phase, the additional turbulence due to the second

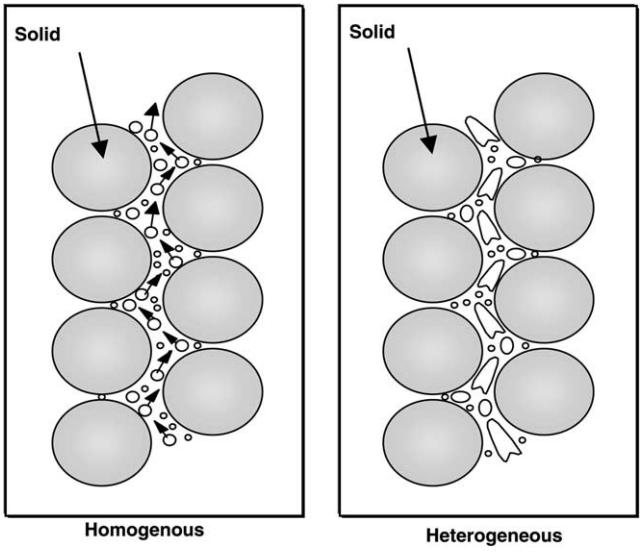

Fig. 4. Sketches of flow in homogeneous and heterogeneous flow regimes.

phase is only small. In this regime, the bubble diameter is generally determined by pore size, surface tension and buoyancy (Lydersen, 1989):

$$d_b = m\left(\frac{d_p \cdot \sigma}{g(\rho_l - \rho_g)}\right)^{1/3} \tag{4}$$

For bubble columns, d_p is the orifice diameter of the gas distributor and $m = 1$. For homogeneous flow in porous media, a value of $m = 0.09$ has been obtained from the analysis of the experimental data. Replacing pore diameter d_p in terms of particle size d_s (see Eq. (9)) gives:

$$d_b = 0.09\left(\frac{\sigma \cdot d_s \cdot \delta}{g \cdot \rho_l \cdot (1-\delta)}\right)^{1/3} \tag{5}$$

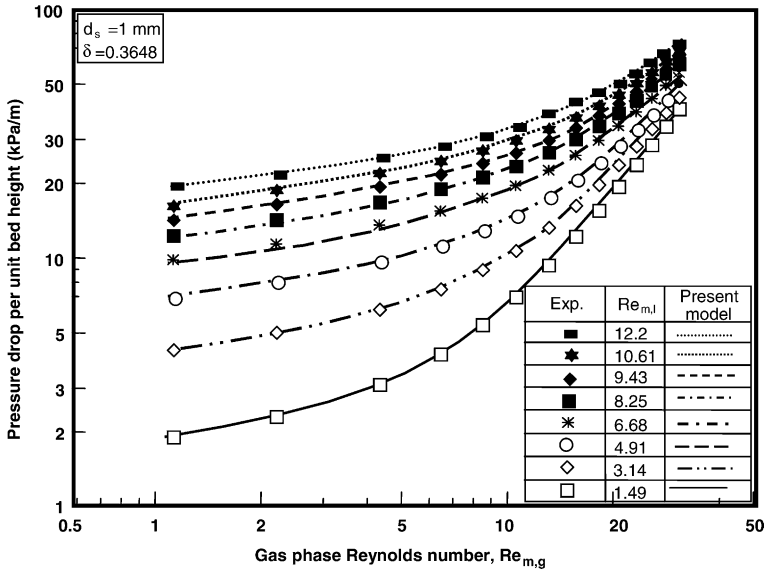

Fig. 5. Experiment and predicated of two-phase pressure drop as a function of gas phase Reynolds number.

In the heterogeneous flow regime, bubbles coalescence within a few centimeters after entering the porous medium at the bottom, to form large longitudinal bubbles. In the present investigation, it was found that

$$\frac{L_b}{d_b} \approx 6\text{–}10 \tag{6}$$

Eq. (6) is in agreement with the findings of Tung and Dhir (1988). The large bubbles occupy almost the whole cross-section of the pores and create significant turbulence and mixing effects, since they flow considerably faster than the liquid phase.

3.2.2. Pressure drop

Only limited published information is available on pressure drop for two-phase flow in porous media, and no generally accepted prediction model has yet been produced. Fig. 5 shows the effect of the modified gas phase Reynolds number $Re_{m,g}$ on the measured two-phase pressure drop for a bed of 1 mm particles, with the modified liquid phase Reynolds number $Re_{m,l}$ as parameter. At each liquid flow rate two regimes can be observed, according to the influence of Reynolds number on the pressure drop. At low gas velocities (i.e. homogeneous flow regime) the pressure drop depends only moderately on the gas phase Reynolds number. In this regime the interaction between bubbles and liquid is negligible and hence the turbulence and mixing are low. At higher gas velocities (i.e. heterogeneous regime) the interaction between bubbles is high, leading to the formation of large bubbles and the associated turbulence/mixing effects. The measurements also show that the effect of liquid phase flow rate is more pronounced for the homogeneous regime than for the heterogeneous regime and that it loses its importance as the gas flow rate increases. The pore-scale flow mechanisms and their relationship to the mean liquid phase saturation can be found elsewhere (Avraam and Payatakes, 1995).

Some of the more widely used correlations available in the literature for prediction of pressure drop during two-phase flow in porous media are compiled in Table 3. Their predictions are compared with the experimental data for a bed packed with 0.5 mm diameter particles in Fig. 6. In most cases, there are considerable discrepancies between the predicted and measured values. As far as the supporting data for these models are concerned, they are confined to a very narrow range of system geometry as well as operating parameters (Izadpanah, 1999), and this may be one of the main reasons why the predicted results are so scattered. The best agreement between measured and predicted values is obtained with the correlation suggested by Larkins and White (1961). This correlation can predict the present experimental data with an absolute mean average error of 28%.

3.2.3. Gas hold-up

Gas hold-up plays two major roles in the evaluation of the transport phenomena in porous media: (i) it provides the volume fraction of the phases present in the system and hence their residence time; (ii) the gas hold-up in conjunction with knowledge of the mean bubble diameter allows the determination of the gas/liquid interfacial area. Typical gas hold-up measurements for a bed of 1 mm particles are shown in Fig. 7 as a function of superficial gas velocity and liquid phase velocity. Again, homogeneous and heterogeneous flow may be distinguished. In the homogeneous regime, gas hold-up

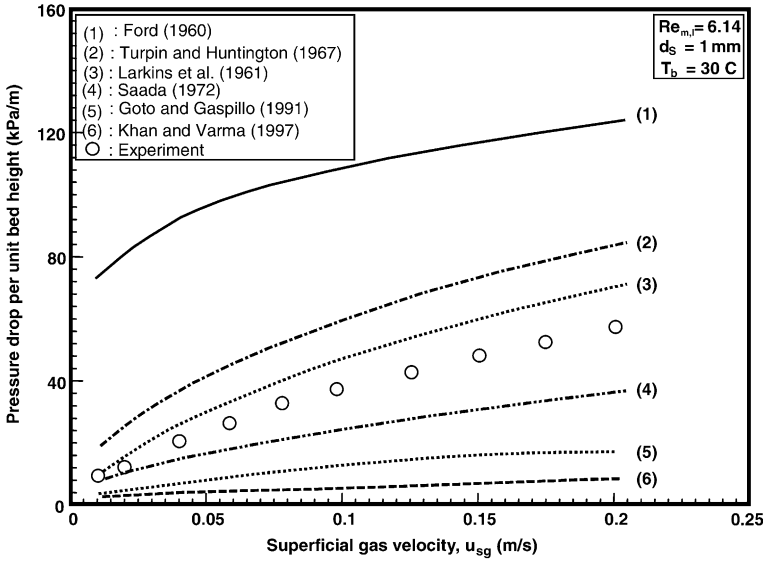

Fig. 6. Prediction of two phase pressure drop from various correlation.

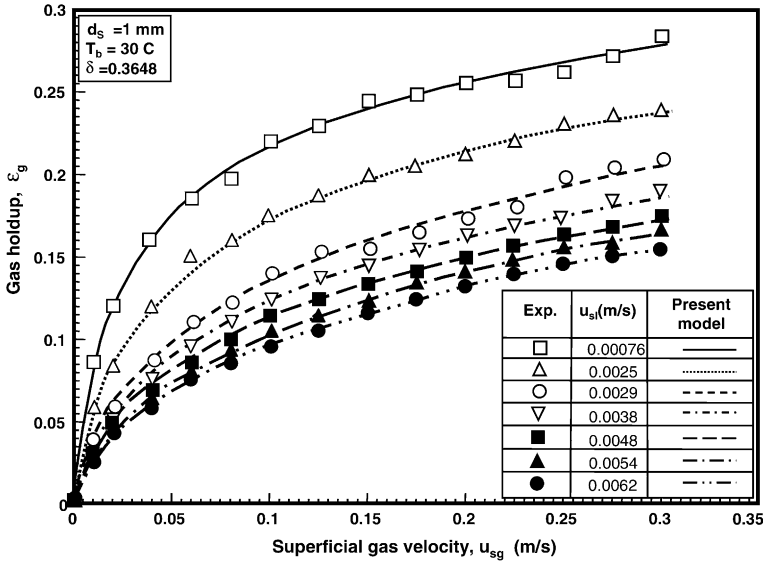

Fig. 7. Experimental and predicated gas holdup as a function of superficial gas velocity.

increases rapidly as gas velocity increases, whereas in the heterogeneous regime this effect is considerably less pronounced. It is important to note that gas hold-up is significantly decreased as the liquid velocity is increased. The liquid phase, which is the wetting phase, takes up the free space in the porous medium; hence less space would be available for the gas phase as the liquid flow rate increases. Furthermore, at higher liquid flow rates, the gas bubbles will wash out of the pores faster, which results in lower gas hold-up. Gas and liquid phase velocities have also a strong effect on the flow regime. It is essential to know the range of parameters over which a particular flow regime prevails and the conditions under which the transition occurs. Transition from homogeneous to heterogeneous flow occurs when the density of the bubbles in the pore space increases to such an extent that the interaction and coalescence between bubbles becomes important.

Several correlations have been suggested for the prediction of gas hold-up in porous media. These correlations are summarized in Table 4. A typical comparison between the measured and predicted gas hold-up values is shown in Fig. 8. While the best trend is obtained from the correlation suggested by Larkins and White (1961) the deviation between the predictions of the various correlations and the measured data is quite considerable.

Table 4
Correlations for the prediction of gas and liquid hold-up

Reference	Correlation	Range of application
Larkins and White (1961)	$\log_{10}\varepsilon_l = -0.774 + 0.525(\log_{10}\chi) - 0.192(\log_{10}\chi)^2$	$0.375 \leqslant \delta \leqslant 0.52$
Turpin and Huntington (1967)	$\varepsilon_l = -0.035 + 0.182\left(\frac{L}{G}\right)^{1.04}$	$1 \leqslant \left(\frac{L}{G}\right)^{0.24} \leqslant 6$
Goto and Gaspillo (1992)	$\ln\frac{\varepsilon_l}{\delta} = -0.442(\ln\chi)^2 + 0.386\ln\chi - 0.178$	Not specified
Saada (1972)	$\varepsilon_l = K\left(\frac{Re}{Re_g}\right)^a$ with transition point at $Re_g^* = 0.44Re_l^2\left(\frac{d_s}{d_c}\right)^{0.38}$ Below transition point: $K = 0.48$ and $a = 1.25$ Above transition point: $K = 0.32$ and $a = 0.07$	Both bubbly and churn turbulent flow regimes

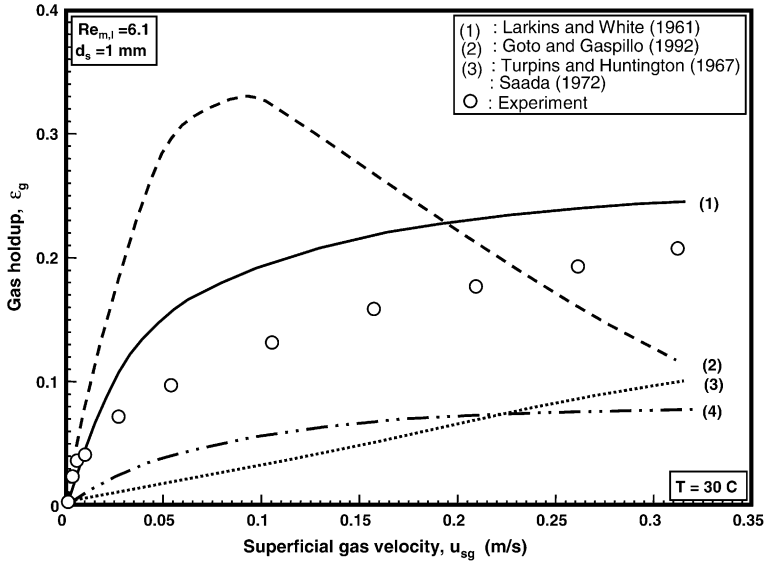

Fig. 8. Prediction of gas holdup from various correlations.

The reason for the differences between the various correlations is mainly due to the experimental procedure, physical properties of the solid phase, system geometry and operating range of the gas and liquid flow rates as well as the correlating procedure of the experimental data.

3.3. Heat transfer coefficient

Fig. 9 shows a typical variation of the heat transfer coefficient with heat flux for an inlet temperature of 30 °C, at two different locations along the bed. The results show that the heat transfer coefficient is independent of the heat flux in the range of the operating conditions used in this investigation. Therefore, it may be concluded that the effect of natural convection is indeed negligible and that forced convection is the main mechanism of heat transfer. The effect of the modified Reynolds number on the single-phase, liquid heat transfer coefficient is shown in Fig. 10, for two locations along the bed and a constant heat flux of 5000 W/m^2. For comparison, the control run for the empty tube is also included. The results show that the heat transfer coefficient increases with increasing liquid phase flow rate and that this effect is considerably more pronounced in the porous medium than in the empty tube. This observation is in agreement with several published investigations (e.g. Varahasamy and Fand, 1996) which report that the enhancement achieved in packed tubes is about 2–7 times the value for unpacked tubes for laminar flow and 2–2.5 times for turbulent flow.

The effect of liquid and gas flow velocity on heat transfer coefficient is shown in Fig. 11 where the heat transfer coefficient is plotted as a function of gas velocity for several liquid flow rates, and a bed of 1 mm particles. It is evident that the heat transfer coefficient passes through a shallow minimum as the gas flow velocity is increased. This change in trend could be attributed to the fact that as the gas flow rate increases, the gas hold-up increases and therefore more void space is occupied by air, hence reducing the wetted surface available to the heat transfer process. Further increase in the gas flow rate increases the number of bubbles until a state is

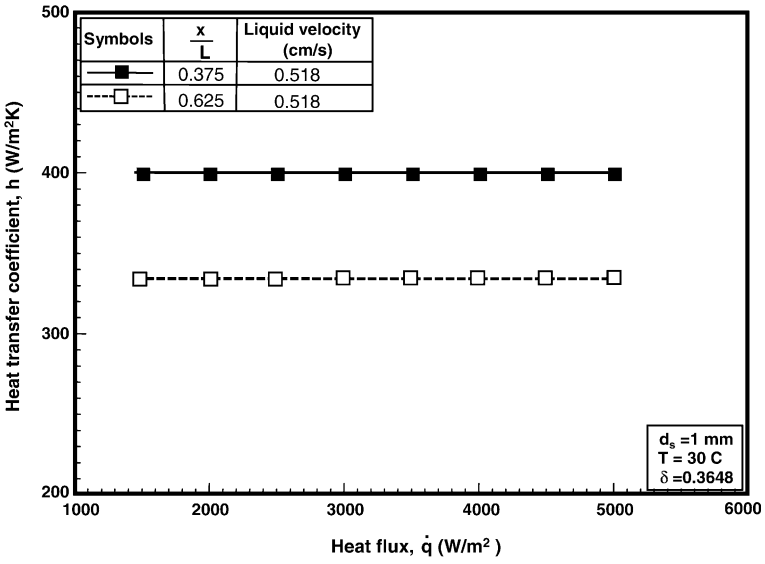

Fig. 9. Heat transfer coefficient as a function of heat flux.

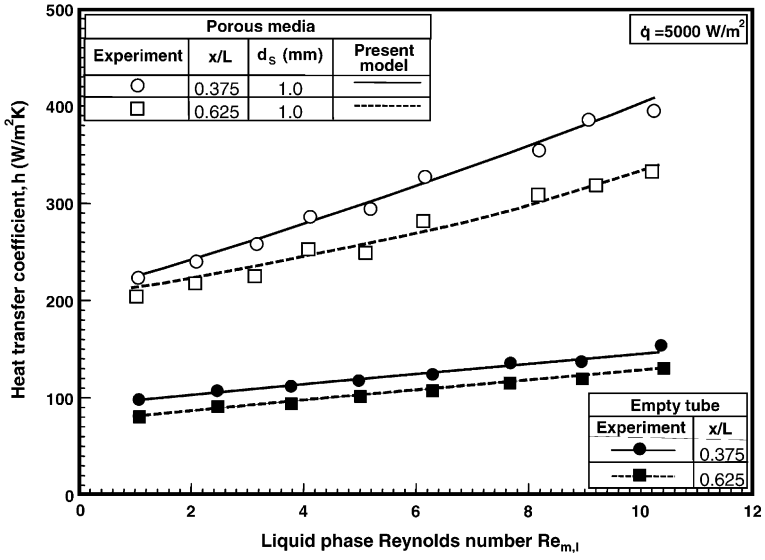

Fig. 10. Variation of heat transfer coefficient as a function of liquid phase Reynolds number.

reached where the bubbles coalesce and larger bubbles are formed. The newly formed bubbles ascend faster in an irregular path through the liquid phase. As these large bubbles move through the bed, they cause some radial movement of the liquid phase which encourages radial mixing leading to the rise in heat transfer coefficient in the heterogeneous regime. It is worthwhile to note that the point at which the graph shows a change in its trend coincides with the transition point of the gas hold-up graph that indicates the change in flow pattern from the homogeneous to the heterogeneous regime. Fig. 12 has been plotted to demonstrate this point. In this figure the variation of gas hold-up and heat transfer coefficient is presented as a function of superficial gas velocity for a particle diameter of 1 mm and a liquid velocity of 0.62 cm/s. It is interesting to compare the shapes of the two curves and the underlying phenomena. In the homogeneous flow regime, heat transfer coefficients decreases gradually to a minimum. Following the transition from homogeneous to heterogeneous flow, this trend is reversed and replaced by a considerable increase in heat transfer coefficient with gas velocity. In the homogeneous flow regime, no significant increase in turbulence occurs and the main effect of the introduction of the tiny bubbles is to reduce the effective thermal conductivity of the bed and, therefore, the heat transfer

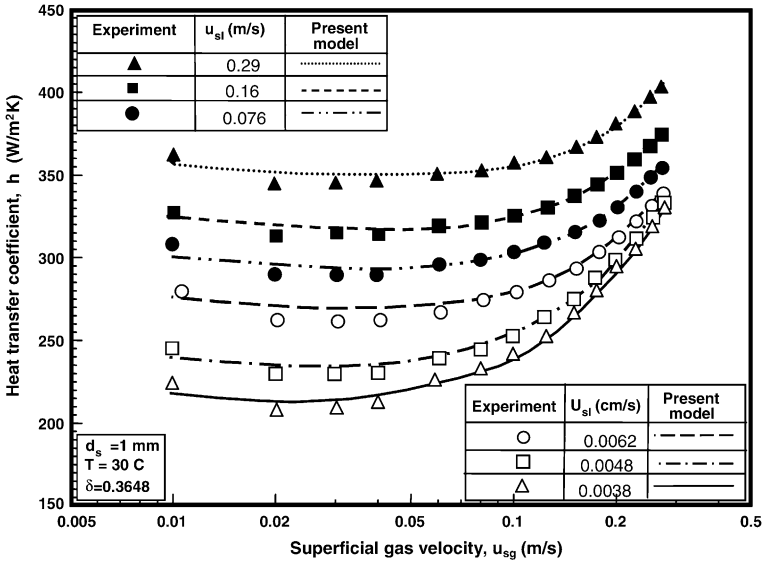

Fig. 11. Experimental and predicated two-phase heat transfer coefficient as a function of superficial gas velocity.

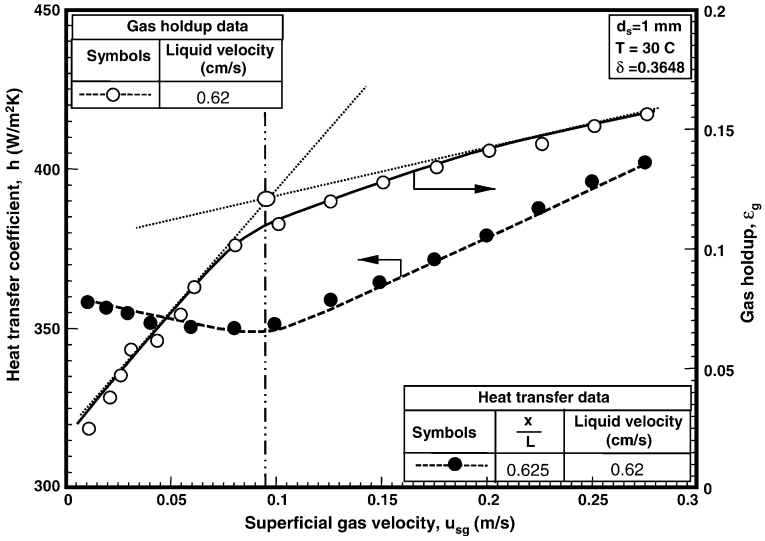

Fig. 12. Variation of heat transfer coefficient and corresponding gas holdup with superficial gas velocity.

coefficient. In the heterogeneous flow regime, the large bubbles or slugs ascend faster and produce additional turbulence. This turbulence and the associated intensified mixing in the liquid phase causes the heat transfer coefficient to increase. As the liquid velocity is increased, the transition from homogeneous to heterogeneous flow occurs at higher gas velocity (see Fig. 11). This is due to the rise in the liquid hold-up, which also delays the change in the flow regime.

The effect of particle size on the heat transfer coefficient is shown in Fig. 13 where the heat transfer rate in beds packed with particles of different sizes are compared at constant liquid velocity of 0.1 cm/s. Particle size is one of the most important parameters affecting the heat transfer coefficient. The heat transfer coefficients increase with increasing particle size, probably due to the increase in gas and liquid hold-up resulting from higher bed porosity. The results also indicate that in the heterogeneous flow regime, the heat transfer coefficient depends strongly on the particle size while in the homogeneous flow regime, this dependency is weak. However, all curves seem to converge into a single line for very small particles. This result is in agreement with the finding of Varahasamy and Fand (1996), which reported that the heat transfer coefficient in packed beds increases as the enhancement ratio d_c/d_s decreases under the same operating conditions.

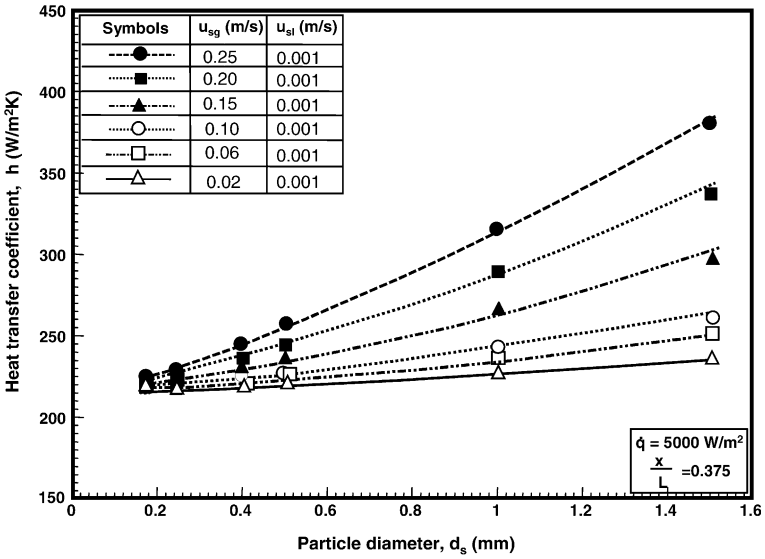

Fig. 13. Effect of particle diameter on two-phase heat transfer coefficient.

4. Correlation of experimental data

4.1. Pressure drop

For flow of an incompressible fluid in a pore of length L and diameter d_p, the pressure drop resulting from the frictional force at the wall is (Coulson and Richardson, 1977a):

$$\frac{\Delta P_f}{L} = \frac{4}{d_p}\left(\frac{f}{2}\right)\cdot \rho u_p^2 \tag{7}$$

The fluid velocity in the pore, u_p can be related to the fluid velocity in the bed as (Coulson and Richardson, 1977b):

$$u_p = \frac{u_f}{\delta} \tag{8}$$

where δ is the porosity of the bed. On the other hand, using a cylindrical pore model, it can be shown that the following relationship also exists between bed porosity, pore diameter and specific surface area of the bed (Izadpanah, 1999):

$$d_p = \frac{\delta d_s}{1.5(1-\delta)} \tag{9}$$

Replacing Eqs. (8) and (9) into Eq. (7) yields:

$$\frac{\Delta P_f}{L} = \frac{f}{2}\cdot\frac{6(1-\delta)}{d_s\delta^3}\cdot\rho_f u_f^2 \tag{10}$$

Equating Eq. (10) with Eq. (3) and solving for friction factor leads to:

$$\frac{f}{2} = \frac{25}{Re_f} + 0.292 \tag{11}$$

The values for single-phase flow pressure drop predicted from Eq. (10) in conjunction with Eq. (11) are compared with experimental data and with the predictions of other models in Fig. 3. As expected the results are in excellent agreement with experimental data and with the prediction of the Kozeny-Carman model.

Two-phase frictional pressure drop in porous media is difficult to predict analytically. Therefore, it is generally determined empirically or by analogies to single-phase flow. Eq. (10) can be extended to two-phase flow in porous media with the appropriate definition of u_f in terms of superficial gas velocity in the porous medium.

$$\frac{\Delta P_t}{L} = \frac{f_t}{2}\cdot\frac{6(1-\delta)}{d_s\delta^3}\cdot\rho_g u_{sg}^2 \tag{12}$$

The two-phase friction factor f_t is a function of gas and liquid phase Reynolds numbers and can be determined from experimental data. For this purpose a data bank containing a large number of data points was compiled over a wide range of operating conditions. These data have been used to develop the following correlation

$$\frac{f_t}{2} = 94\left(\frac{Re_l^{1.11}}{Re_g^{1.8}}\right) + 4.4 \tag{13}$$

The applicability of Eq. (12) in conjunction with Eq. (13) for prediction of two-phase flow through porous media is demonstrated in Fig. 5 where the experimental results are also compared with values predicted from Eq. (12). The absolute mean average error between measured and predicted values is about 5.6%, which demonstrates the applicability of the suggested model.

4.2. Gas hold-up

Gas hold-up is a function of particle size, bubble size, gas and liquid phase superficial velocities. In analogy to

two-phase gas/liquid flow in tubes this functionality can be expressed in the following form (Lapidus and Elgin, 1957):

$$\frac{\varepsilon_g}{\delta-\varepsilon_g}=F(u_r,d_r) \tag{14}$$

Solving Eq. (14) for gas hold-up yields

$$\varepsilon_g=\frac{\delta\cdot F(u_r,d_r)}{1+F(u_r,d_r)} \tag{15}$$

where

$$u_r=\frac{u_{sg}}{u_{sl}}\quad\text{and}\quad d_r=\frac{d_b}{d_s} \tag{16}$$

Eq. (5) shows that

$$d_r\propto\frac{\delta}{1-\delta} \tag{17}$$

Non-linear regression analysis is used to find the functionality $F(u_r,d_r)$ from the present gas hold-up experimental data. The result of these calculations shows that

$$F(u_r,d_r)=u_r^{0.675}\left(\frac{\delta}{1-\delta}\right)^{5.24} \tag{18}$$

The predictions of Eq. (15) in conjunction with Eq. (18) are also compared with experimental data in Fig. 7 over a wide range of gas and liquid flow rates. The absolute mean average error between the predicted and experimental data is only about 4.2%.

4.3. Single-phase heat transfer coefficient

The volume-averaged two-dimensional steady-state equation of energy in cylindrical coordinates in porous media is

$$\frac{\partial^2T}{\partial r^2}+\frac{1}{r}\frac{\partial T}{\partial r}-\frac{u_f}{\alpha_e}\frac{\partial T}{\partial x}=0 \tag{19}$$

The initial and boundary conditions of Eq. (19) in the present investigation are

$$T_{r,0}=T_0,\quad\frac{\partial T}{\partial r_{0,x}}=0\quad\text{and}\quad\frac{\partial T_{r_0,x}}{\partial r}=\frac{\dot q}{\lambda_{os}} \tag{20}$$

Analytical solution of Eq. (19) subject to the above conditions yields

$$T_{s(r_0,x)}=T_0+\frac{2\alpha_e\dot q}{u_f\lambda_{os}r_0}x+\frac{\dot q r_0}{4\lambda_{os}}+J_0(\Lambda_n,r_0)\times\sum_{n=1}^{\infty}C_n e^{-\frac{\alpha_e\Lambda_n^2x}{u_f}} \tag{21}$$

$$T_{s(0,x)}=T_0+\frac{2\alpha_e\dot q}{u_f\lambda_{os}r_0}x-\frac{\dot q r_0}{4\lambda_{os}}+\sum_{n=1}^{\infty}C_n e^{-\frac{\alpha_e\Lambda_n^2x}{u_f}} \tag{22}$$

Therefore, the heat transfer coefficient becomes

$$h=\frac{1}{\frac{r_0}{4\lambda_{os}}+J_0(\Lambda_n,r_0)\sum_{n=1}^{\infty}C_n e^{-\frac{\alpha_e\Lambda_n^2}{u_f}x}} \tag{23}$$

where

$$C_n=\frac{2\dot q\cdot J_2(\Lambda_n,r_0)}{J_0^2(\Lambda_n,r_0)\cdot\lambda_{os}\cdot r_0\cdot\Lambda_n^2} \tag{24}$$

The stagnant thermal conductivity, λ_{os} is given by Nield (1991) as:

$$\lambda_{os}=\lambda_s^{1-\delta}\cdot\lambda_f^{\delta} \tag{25}$$

A comparison between measured and predicted heat transfer coefficient from Eq. (23) is shown in Fig. 10 as a function of fluid Reynolds number at constant heat flux. The calculated trends are in excellent agreement with the experimental data. Eq. (23) predicts all the experimental data obtained for single-phase flow under various operating conditions with absolute mean average error of 6%.

4.4. Two-phase heat transfer coefficient

The partial differential equation of energy for the cylindrical section of a porous medium with co-current gas and liquid flow is given as (Weekman and Myers, 1965; Izadpanah, 1999):

$$\left(\varepsilon_g\rho_g u_{sg}c_{pg}+(1-\varepsilon_g)\rho_l u_{sl}c_{pl}\right)\frac{\partial T}{\partial x}=\lambda_{et}\left(\frac{1}{r}\frac{\partial T}{\partial r}+\frac{\partial^2T}{\partial r^2}\right) \tag{26}$$

where λ_{et} is the effective thermal conductivity which lumps all resistances to heat transfer. These resistances include the thermal resistance at the wall and the thermal resistances between the phases. Eq. (26) can be simplified to

$$\frac{\partial^2T}{\partial r^2}+\frac{1}{r}\frac{\partial T}{\partial r}-\frac{u_{sl}}{\Gamma}\frac{\partial T}{\partial x}=0 \tag{27}$$

where

$$\Gamma=\frac{\lambda_{et}u_{sl}}{\varepsilon_g\rho_g c_{pg}u_{sg}+(1-\varepsilon_g)\rho_l c_{pl}u_{sl}} \tag{28}$$

Eq. (27) is subject to the following initial and boundary conditions:

$$T_{r0}=T_0,\quad\left.\frac{\partial T}{\partial r}\right|_{r=0}=0\quad\text{and}\quad\left.\frac{\partial T}{\partial r}\right|_{r=R_0}=\frac{\dot q}{\lambda_{et}} \tag{29}$$

Analytical solution of Eq. (27) with conditions defined by Eq. (29) yields:

$$h_t=\left[\frac{r_0}{4\lambda_{et}}+\sum_{n=1}^{\infty}C_n\exp\left(-\frac{\Lambda_n^2\Gamma}{u_D}x\right)J_0(\Lambda_nR_0)\right]^{-1} \tag{30}$$

The only factor, which needs to be evaluated in Eq. (30), is λ_{et}, which is defined by most investigators as:

$$\lambda_{et} = \lambda_{dt} + \lambda_{ot} \tag{31}$$

Dispersion thermal conductivity, λ_{dt}, is the sum of dispersion conductivity arising from the movement of the two phases in the porous medium and can be expressed as (Wang and Beckerman, 1993):

$$\lambda_{dt} = (1-\varepsilon_g)\gamma_l \rho_l c_{pl} d_p u_{sl} + \varepsilon_g \gamma_g \rho_g c_{pg} d_p u_{sg} \tag{32}$$

The values of the constants γ_l and γ_g are to be found experimentally. The stagnant thermal conductivity, λ_{ot}, can be obtained by modification of Eq. (25) by the inclusion of the gas hold-up to yield:

$$\lambda_{ot} = \lambda_s^{1-\delta}\left[(1-\varepsilon_g)\lambda_l + \varepsilon_g \lambda_g\right]^{\delta} \tag{33}$$

The predictions of Eq. (30) for a bed packed with 1 mm particles at several liquid velocities have been included as solid lines in Fig. 11. The calculated trends are in excellent accordance with the experimental results over a wide range of superficial gas velocities. Furthermore, Eq. (30) predicts a minimum heat transfer coefficient at a gas velocity of about 10 cm/s which is in good agreement with the experimental data. The applicability of the presented model for the prediction of two-phase flow heat transfer in porous media is demonstrated in Fig. 14 where about 800 experimental data are compared with the corresponding predictions from Eq. (30). The absolute mean average error between the predictions of the model and the experimental data is about 7%.

5. Conclusions

A mathematical model based on the volume-average energy equation has been developed to predict temperature distribution and single-phase heat transfer coefficient. Comparison of the predicted values with experimental data shows a good agreement. The model can be used confidently to predict the single-phase heat transfer coefficient in cylindrical porous media under constant wall heat flux conditions. The experimental observations of gas/liquid flow through porous media suggest the existence of two distinct flow regimes, namely homogeneous and heterogeneous flow. While the homogeneous regime is characterized by the presence of small rigid spherical bubbles, the heterogeneous regime features large bubbles traveling at relatively high velocities. Analysis of experimental results has shown the dependency of gas hold-up on bubble size, fluid velocities and bed particle size. A new correlation is presented for the prediction of gas hold-up which can predict the experimental data with good accuracy. The capillary pore model is used to model flow pressure drop in porous media. Then, this model is extended to develop a reliable model for the prediction of two-phase pressure drop. Significant improvement in heat transfer coefficient was observed due to the presence of bubbles in the porous media. In the homogeneous flow regime, the heat transfer coefficient slightly decreases with increasing gas velocity. However, once the flow regime has changed from homogeneous to heterogeneous flow, significant improvement in heat transfer coefficient was observed. Finally, a model is proposed for the prediction of convective heat transfer coefficients in two-phase gas/liquid flow through porous media. This model, which is obtained from the modification of single-phase heat

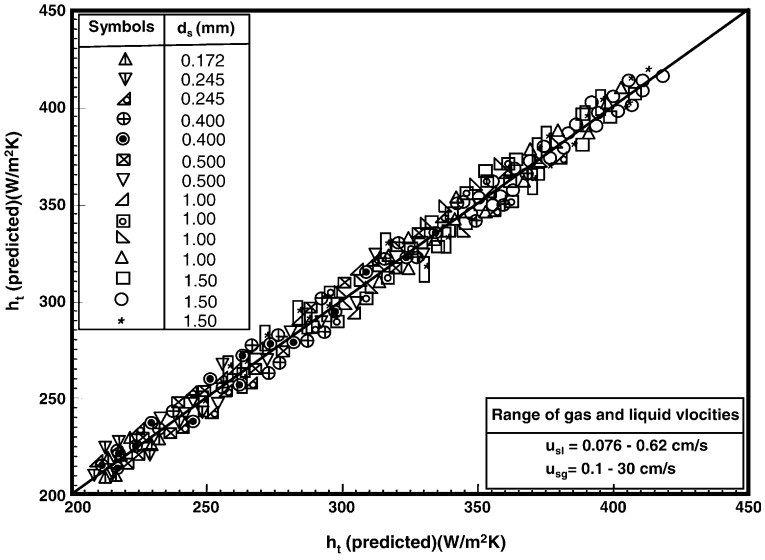

Fig. 14. Comparison of measured and predicated two phase heat transfer coefficient.

transfer through porous media, predicts the experimental results with good accuracy.

References

Amiri, A., Vafai, K., 1994. Analysis of dispersion effects and non-thermal equilibrium non-Darcian, variable porosity incompressible flow through porous media. Int. J. Heat Mass Transfer 37, 939–954.

Amiri, A., Vafai, K., Kuzay, T.M., 1995. Effects of boundary conditions on non-Darcian heat transfer through porous media and experimental comparisons. Numer. Heat Transfer 27, 651–664.

Avraam, D.G., Payatakes, A.C., 1995. Flow regimes and relative permeabilities during stead state two-phase flow in porous media. J. Fluid Mech. 293, 207–236.

Bear, J., 1972. Dynamics of Fluid in Porous Media. Elsevier, New York.

Bear, J., Bachmat, Y., 1990. Introduction to Modelling of Transport Phenomena in Porous Media. Kluwer Academic, Dordrecht.

Blake, F.V., 1922. The resistance of packing to fluid flow. Trans. Amer. Inst. Chem. Emgrs. 14, 415–421.

Cheng, P., 1978. Heat transfer in geothermal systems. Adv. Heat Transfer 14, 1–105.

Combarnous, M.A., Bories, S.A., 1975. Hydrothermal convection in saturated porous media. Adv. Hydrosci. 10, 231–307.

Coulson, J.M., Richardson, J.F., 1977a. Chemical Engineering, third ed, vol. 1. Pergamon Press.

Coulson, J.M., Richardson, J.F., 1977b. Chemical Engineering, third ed, vol. 2. Pergamon Press.

Darcy, H., 1856. Les fontaines publiques de la ville de Dyon. Victor Dalmont.

Dinulescu, H.A., Eckert, 1980. Analysis of one dimensional moisture migration caused by temperature gradients in a porous media. Int. J. Heat Mass Transfer 23, 1069–1078.

Dybbs, A., Schweitzer, S., 1973. Conservation equations for non-isothermal flow in porous media. J. Hydrol. 20, 171–180.

Eisenklam, P., Ford, L.H., 1962. On the interaction of fluids and solids. Inst. Chem. Engrs. London, 333–344.

Ergun, S., 1952. Fluid flow through packed columns. Chem. Eng. Progr. 48, 89–105.

Ford, L.H., 1960. Multiphase Flow through Porous Media with Special Reference to Turbulent Region. Ph.D. Thesis, University of London.

Forchheimer, P., 1901. Wasserbewegung durch Böden. Zeitschrift des Vereins Deutscher Ingenieure 45, 1736–1741, and 1781–1788.

Goto, S., Gaspillo, P.A., 1992. Multiple hydrodynamics states in gas-liquid up-flow and down-flow through beds of small packing. Ind. Eng. Chem. Res. 31, 629–632.

Hassanizadeh, S.M., Gray, W.G., 1988. Reply to comments by Barak on "High velocity flow in porous media". Transport Porous Media 3, 319–321.

Hassanizadeh, S.M., Gray, W.G., 1993. Towards an improved description of the physics of two-phase flow. Adv. Water Resour. 16, 53–67.

Hunt, M.L., Tien, C.L., 1988. Non-Darcian convection in cylindrical packed beds. J. Heat Transfer 110, 378–384.

Izadpanah, M.R., 1999. Heat Transfer and Pressure Drop during Single and Two-phase Flow through Unconsolidated Porous Media. Ph.D. thesis, the University of Surrey, Guildford, UK.

Kawiany, M., 2002. Principles of Heat Transfer in Porous Media. Springer-Verlag.

Khan, A.A., Varma, Y.B.G., 1997. Flow identification and pressure drop in co-current gas–liquid up flow through packed beds. Bioprocess Eng. 16, 355–360.

Kozeny-Carman, J., 1927. Über kapillare Leitung des Wassers im Boden. Ber. Wien. Akd. 136, 271–278.

Lapidus, L., Elgin, J.C., 1957. Mechanics of vertical moving fluidized systems. AIChE J. 3, 63–68.

Larkins, R.P., White, R.R., 1961. Two-phase co-current flow in packed beds. AIChE J. 7, 231–239.

Leva, M., 1947. Pressure drop through packed tubes: Part I. A general correlation. Chem. Eng. Progr. 43, 713–717.

Lipinski, R.J., 1981. A one dimensional particle bed dry-out model. ANS Trans. 38, 386–387.

Lyczkowski, R.W., Chao, Y.T., 1984. Comparison of Stefan model with two-phase model of coal drying. Int. J. Heat Mass Transfer 27, 1157–1169.

Lydersen, A.L., 1989. Fluid Flow and Heat Transfer. John Wiley and Sons, pp. 219–220.

Nield, D.A., 1991. Convection in a porous medium with inclined temperature gradient. Int. J. Heat Mass Transfer 34, 87–92.

Nield, D.A., Bejan, A., 1999. Convection in Porous Media. Springer-Verlag, New York.

Nilson, R.H., Romero, L.A., 1980. Self-similar condensing flows in porous media. Int. J. Heat Mass Transfer 23, 1461–1470.

Ogniewicz, Y., Tien, C.L., 1981. Analysis of condensation in porous insulation. Int. J. Heat Mass Transfer 24, 421–429.

Plumb, O.A., Burnett, D.B., Shekariz, A., 1990. Film condensation on a vertical flat plate in a packed bed. ASME J. Heat Transfer 112, 234–239.

Saada, M., 1972. Fluid mechanics of co-current two-phase flow in packed beds: pressure drop and liquid hold-up studies. Chem. Ind. Genie Chem. 105, 1415–1421.

Scheidegger, A.E., 1974. The Physics of Flow through Porous Media. University of Toronto Press, Toronto.

Shah, Y.T., 1979. Gas–Liquid–Solid reactor design. McGraw-Hill, New York.

Sondergeld, C.H., Turcotte, D.L., 1977. An experimental study two-phase convection in a porous medium with applications to geological problems. J. Geophys. Res. 82, 2045–2053.

Sözen, M., Vafai, K., 1990. Analysis of the non-thermal equilibrium condensing flow of a gas through a packed bed. Int. J. Heat Mass Transfer 33, 1247–1261.

Sözen, M., Vafai, K., 1993. Longitudinal heat dispersion in porous beds with real gas flow. AIAA J. Thermophys. Heat Transfer 7, 153–157.

Stankiewicz, A., 1989. Advanced modelling and design of multi-tubular fixed-bed reactor. Chem. Eng. Technol. 12, 113–130.

Tien, C.L., Vafai, K., 1990. Convective and radiative heat transfer in porous media. Adv. Appl. Mech. 27, 225–281.

Tung, V.X., Dhir, V.K., 1988. A hydrodynamic model for two-phase flow through porous media. Int. J. Multiphase flow 14, 47–65.

Turpin, J.L., Huntington, R.L., 1967. Prediction of pressure drop for two-phase two-component co-current flow in packed beds. AIChE J. 13, 1196–1202.

Vafai, K., Sarkar, S., 1987. Heat and mass transfer in partial enclosures. AIAA J. Thermophys. Heat Transfer 1, 253–259.

Vafai, K., Sözen, M., 1990. An investigation of a latent heat storage porous bed and condensing flow through it. ASME J. Heat Transfer 112, 1014–1022.

Vafai, K., Tien, C.L., 1981. Boundary and inertia effects on flow and heat transfer in porous media. Int. J. Heat Mass Transfer 24, 195–203.

Vafai, K., Whitaker, S., 1986. Simultaneous heat and mass transfer accompanied by phase change in porous insulation. ASME J. Heat Transfer 108, 132–140.

Vafai, K., Alkir, R.L., Tien, C.L., 1985. An experimental investigation of heat transfer in variable porosity media. J. Heat Transfer 107, 642–647.

Varahasamy, M., Fand, R.M., 1996. Heat transfer by forced convection in pipes packed with porous media whose matrices are composed of spheres. Int. J. Heat Mass Transfer 39, 3931–3947.

Wang, C.Y., Beckerman, C., 1993. A two-phase mixture model of liquid/gas flow and heat transfer in capillary porous media—I. Formulation. Int. J. Heat Mass Transfer 36, 2747–2758.

Weekman, V.W., Myers, J.E., 1965. Heat transfer characteristics of co-current gas/liquid flow in packed beds. AIChE J. 11, 13–17.

White, S.M., Tien, C.L., 1987a. Analysis of laminar condensation in a porous medium. In: Proc. of the ASME-JSME Thermal Engineering Joint Conference, Honolulu, Hawaii, vol. 2, pp. 401–406.

White, S.M., Tien, C.L., 1987b. Experimental investigation of film condensation in porous structures. In: Proc. of the 6th International Heat Pipe Conference, Fundamental and Basic Research: Theoretical and Experimental Studies, pp. 148–153.

Zhukova, T.B., Pisarenko, V.N., Kafarov, V.V., 1990. Modelling and design of industrial reactors with stationary bed of catalyst and two-phase gas-/liquid—a review. Int. Chem. Eng. 30, 57–102.